Nozzle Study

Yan Zhan, Foluso Ladeinde

April 21, 2011

Outlines

- Region of interests
- Bend Combinations without nozzle
  - Bend Combinations Without Nozzle
  - Turbulence Model Comparisons
  - Mercury Flow in Curved Pipes
  - Discussions
- Bend Combinations with Nozzle
  - Bend Combinations With Nozzle
  - Mercury Flow in Curved Nozzle Pipes
  - Discussions
- Appendix

Region of interests

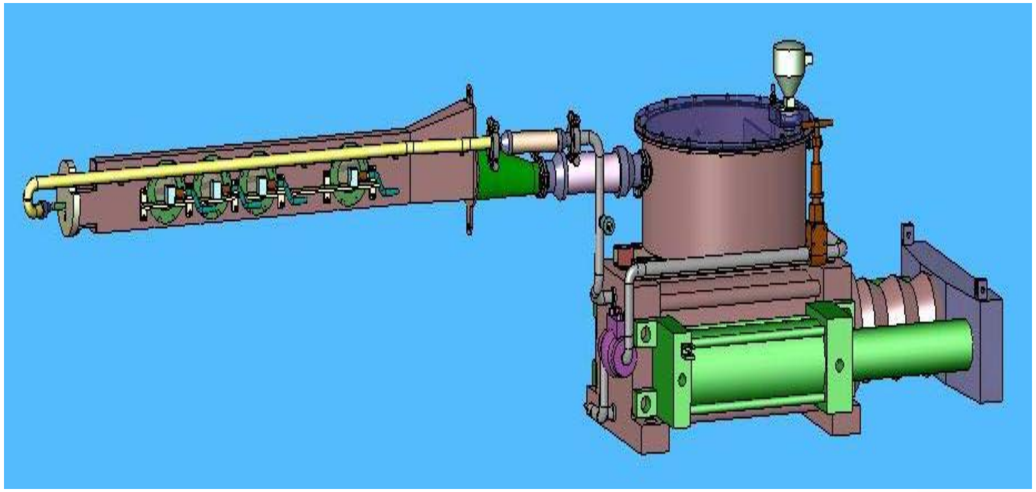

Interests: Influence of nozzle & nozzle upstream on the jet exit

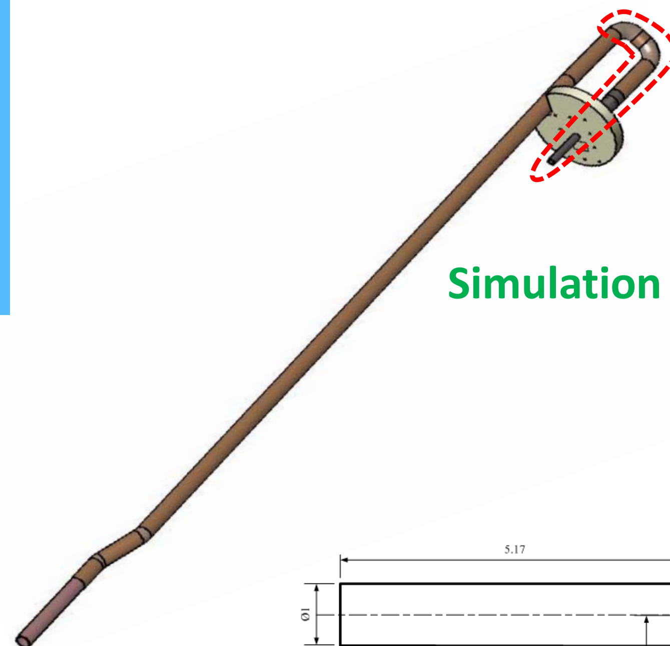

Simulation Regime

Hg delivery system at CERN

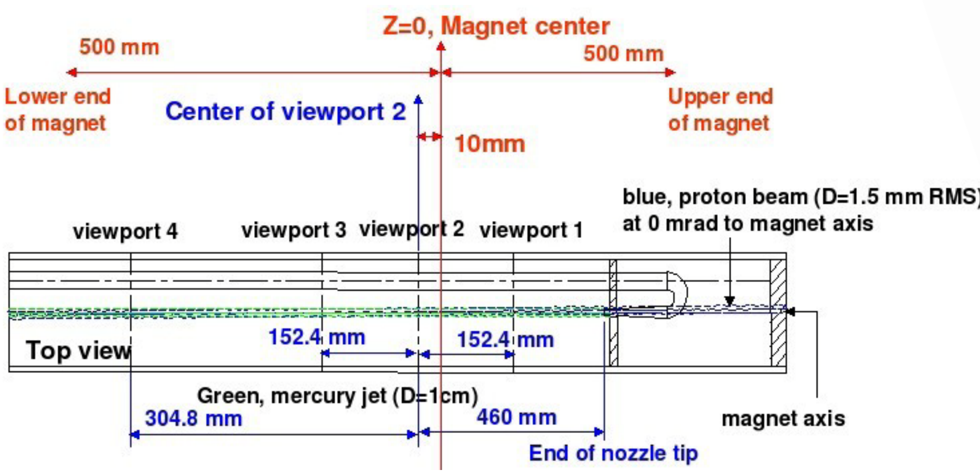

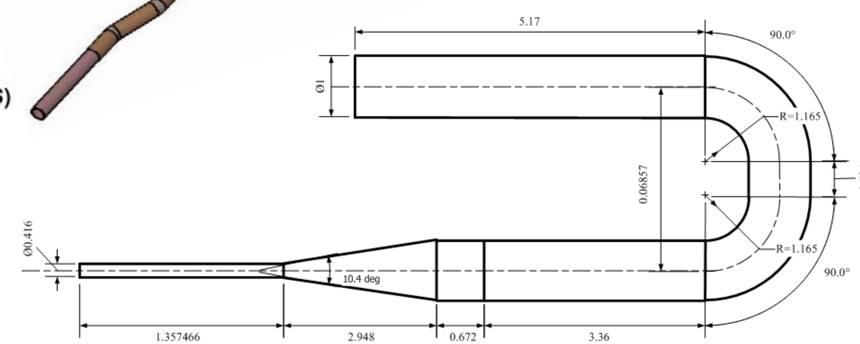

Outlines

- Region of interests
- Bend Combinations without nozzle
  - Bend Combinations Without Nozzle
  - Turbulence Model Comparisons
  - Mercury Flow in Curved Pipes
  - Discussions
- Bend Combinations with Nozzle
  - Bend Combinations With Nozzle
  - Mercury Flow in Curved Nozzle Pipes
  - Discussions
- Appendix

Bend Combinations Without Nozzle (1)

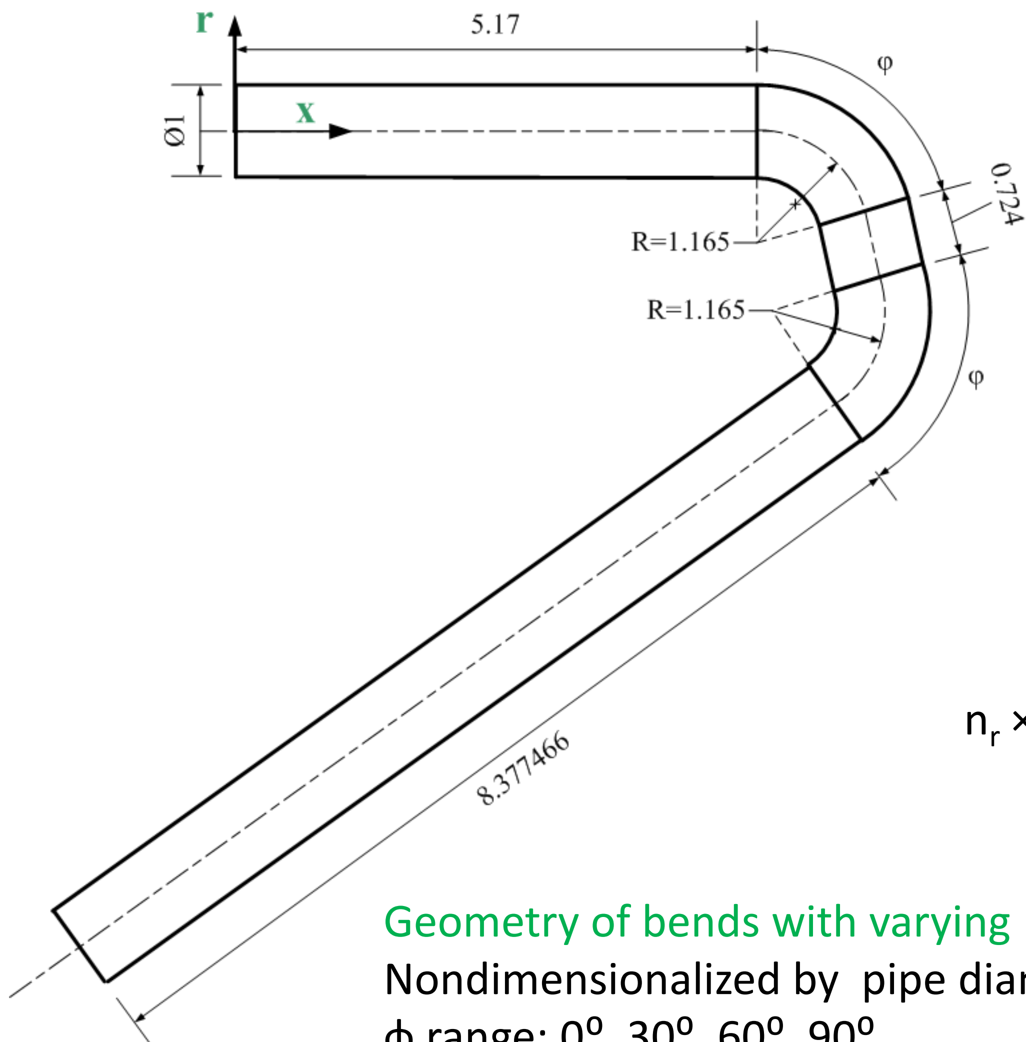

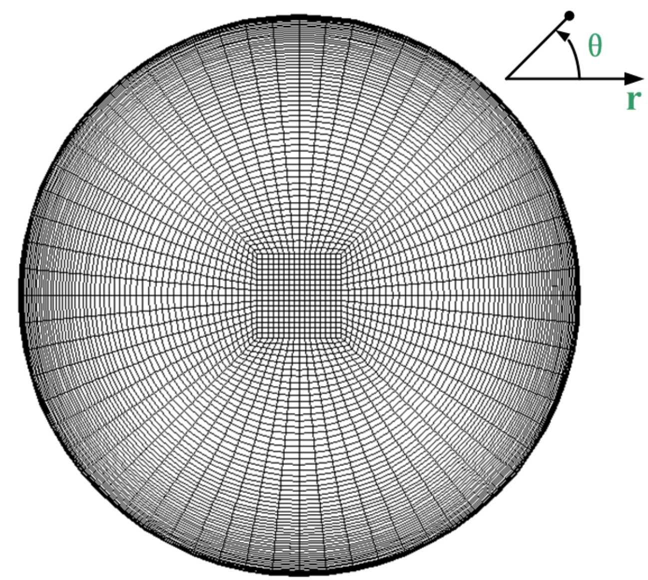

Mesh at the cross-section

$n_r \times n_\theta$ =152×64 (the 1st grid center at $y^+ \approx 1$)

Geometry of bends with varying angles

Nondimensionalized by pipe diameter (p.d.);

ϕ range: 0º, 30º, 60º, 90º.

Bend Combinations Without Nozzle (2)

(a)

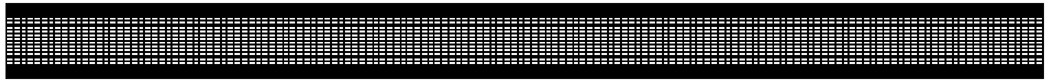

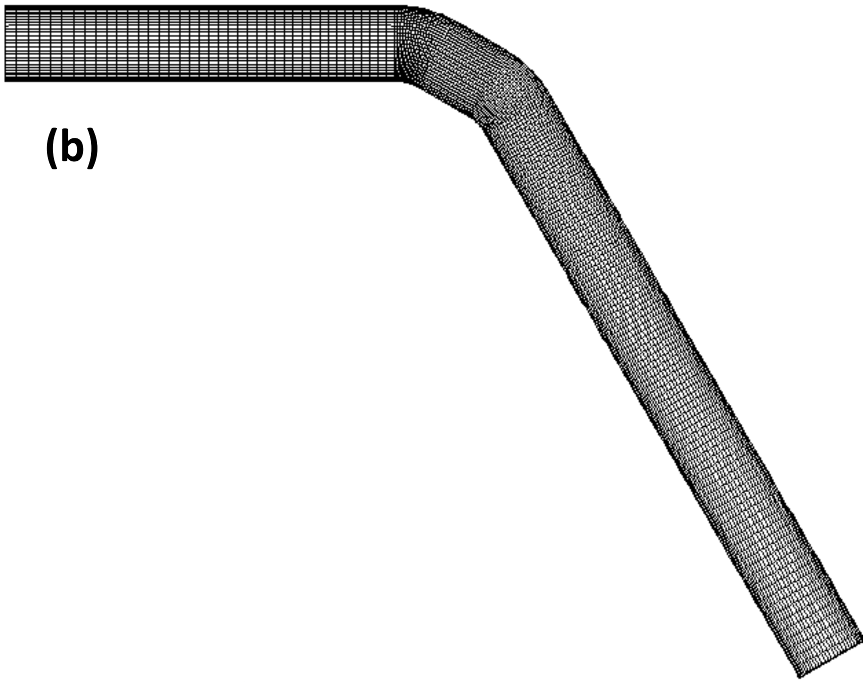

(b)

(c)

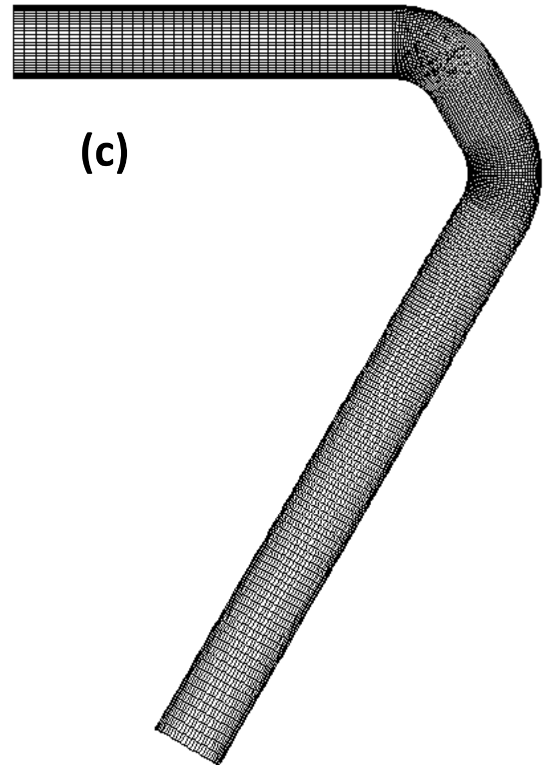

(d)

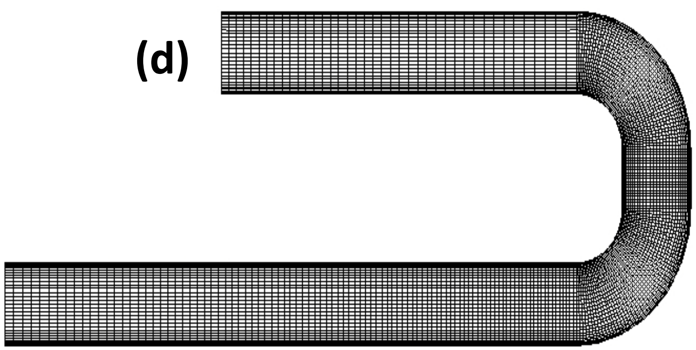

Geometries without nozzle:

(a) $0^\circ/0^\circ$; (b) $30^\circ/30^\circ$; (c) $60^\circ/60^\circ$; (d) $90^\circ/90^\circ$

$n_x = 40 + n_\phi + 20 + n_\phi + 100$

where n_ϕ depends on the bend angle ϕ

Turbulence Model Comparisons (2)

Sudo's Experiment (1998) for 90^{o} bend*

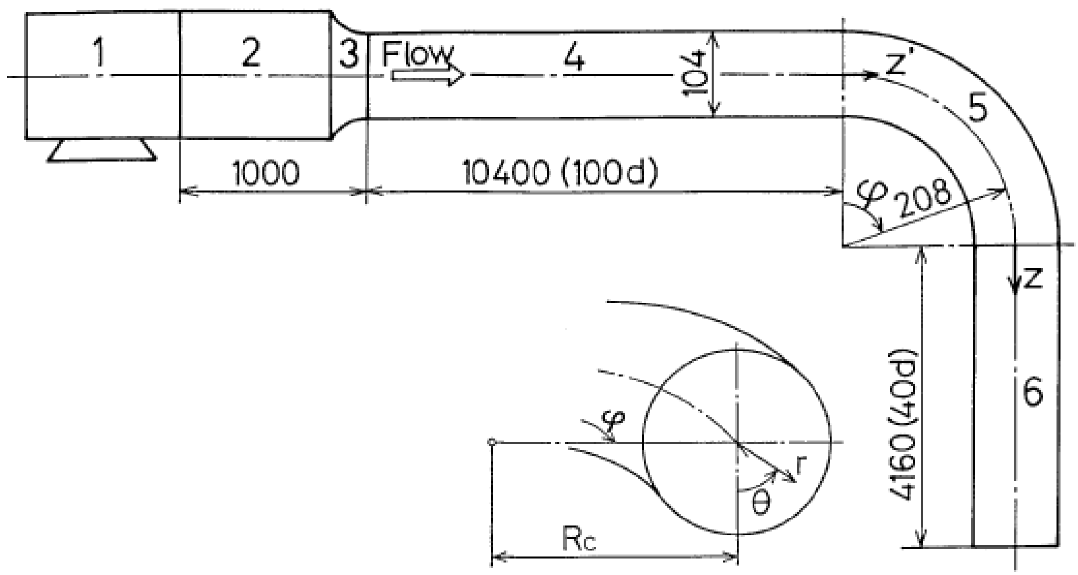

Fig. 1. Schematic diagram of test pipe and coordinate system.
1 Fan; *2* settling chamber; *3* contraction; *4* upstream tangent; *5* 90° bend; *6* downstream tangent

u_{ave} = 8.7 m/s; Re=6×10^{4}; ρ_{air} = 1.2647; μ_{air} = 1.983×10^{-5}; Pr= 0.712

•**K. Sudo, M. Sumida, H. Hibara, 1998. Experimental investigation on turbulent flow in a circular-sectioned 90-degrees bend, Experiments in Fluids. 25, 42-49.**

Turbulence Model Comparisons (3)

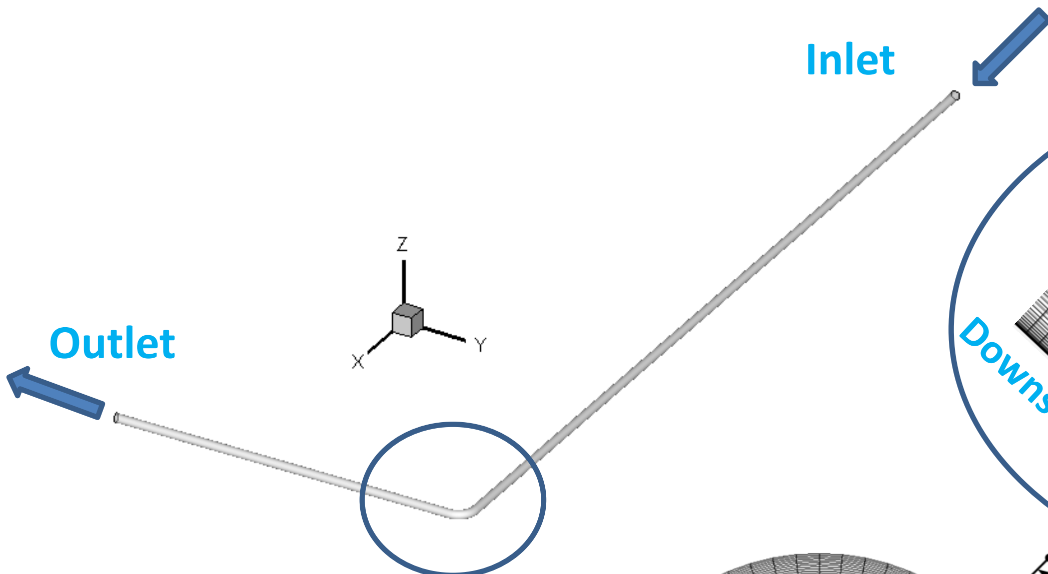

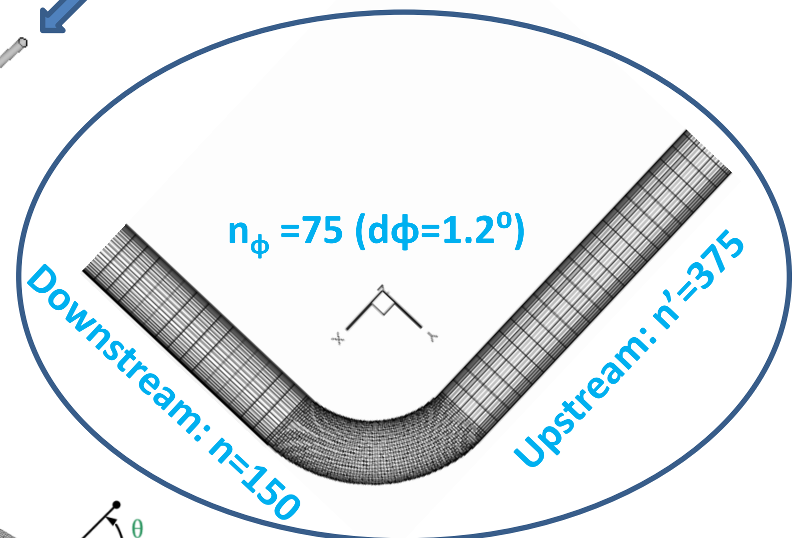

Mesh for the test pipe

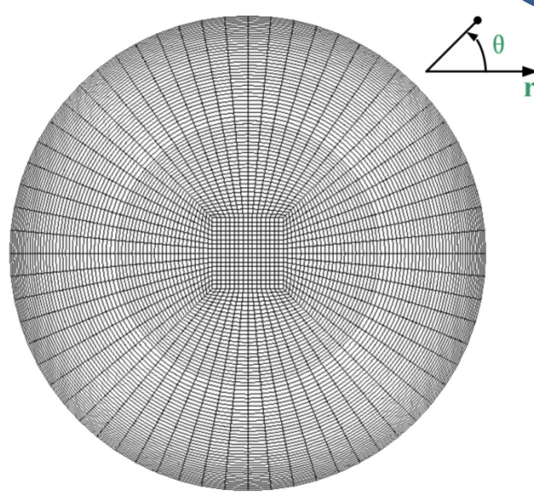

Mesh at the cross-section

$n_r \times n_\theta$ =80×50 (the 1st grid center at $y^+ \approx 1$)

Turbulence Model Comparisons (4)

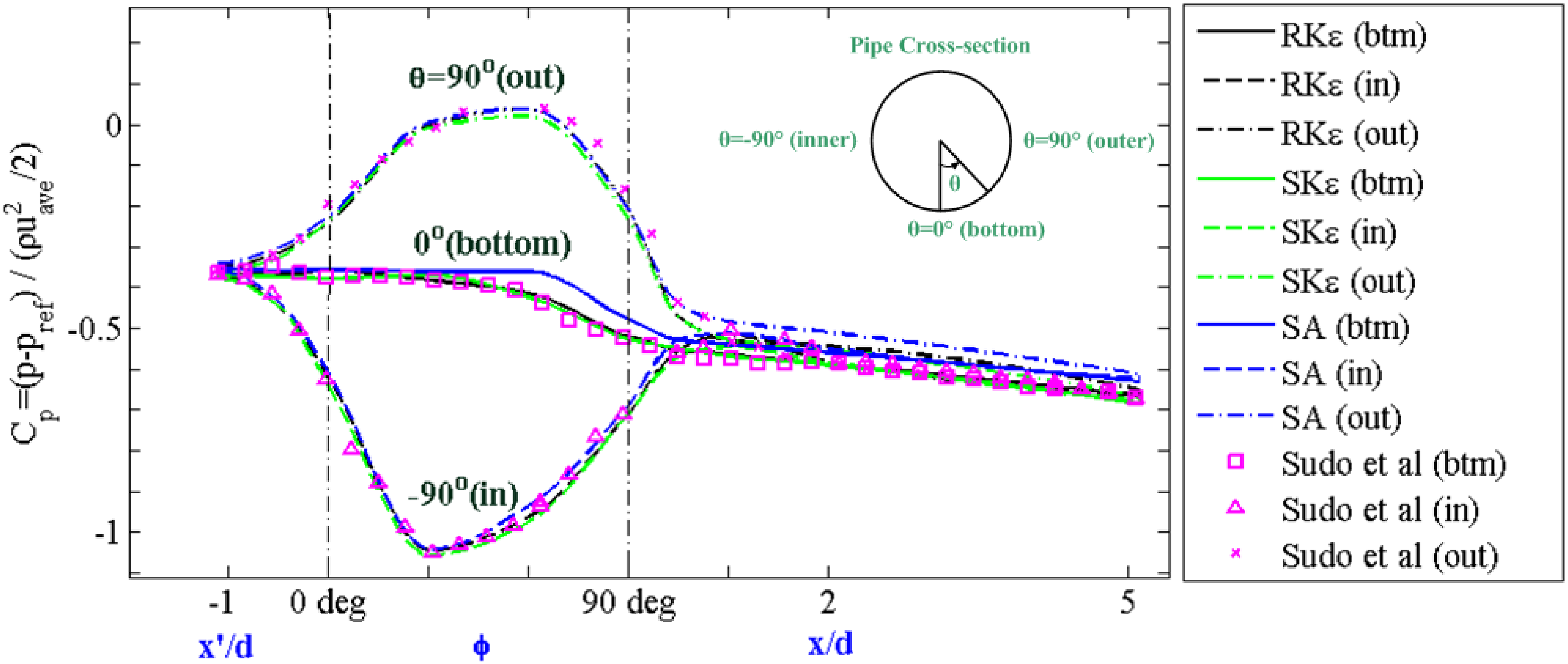

Longitudinal distribution of wall static pressure

C_p pressure coefficient

p_{ref} reference value of p at z'/d=-17.6

RKε is the best of the three in simulating curved pipe flow

Mercury Flow in Curved Pipes (1)

- Steady incompressible turbulent flow
- Boundary Conditions
  - Inlet: Fully developed velocity;
  - Outlet: Outflow;
  - Wall: non-slip
- Schemes
  - 3rd order MUSCL for momentum and turbulence equations
  - SIMPLE schemes for pressure linked equations
- Convergence Criterion
  - 10^{-5}

Mercury Flow in Curved Pipes (2)

- Turbulence Characteristics
  - Turbulence Level (**Flutuating Velocity**)

$$I \equiv \frac{u'}{u_m} = \frac{\sqrt{2k/3}}{u_m}$$

Small *I*

  - Momentum Thickness (**Mean Velocity**)

Measure of the momentum loss within the boundary layer due to viscosity.

$$\rho\theta_t UU = \int_0^R \rho u(U-u)dy \Rightarrow \theta_t = \int_0^R \frac{u}{U}(1-\frac{u}{U})dr$$

Big θ_t

Mercury Flow in Curved Pipes (3)

- Turbulence Level (1)

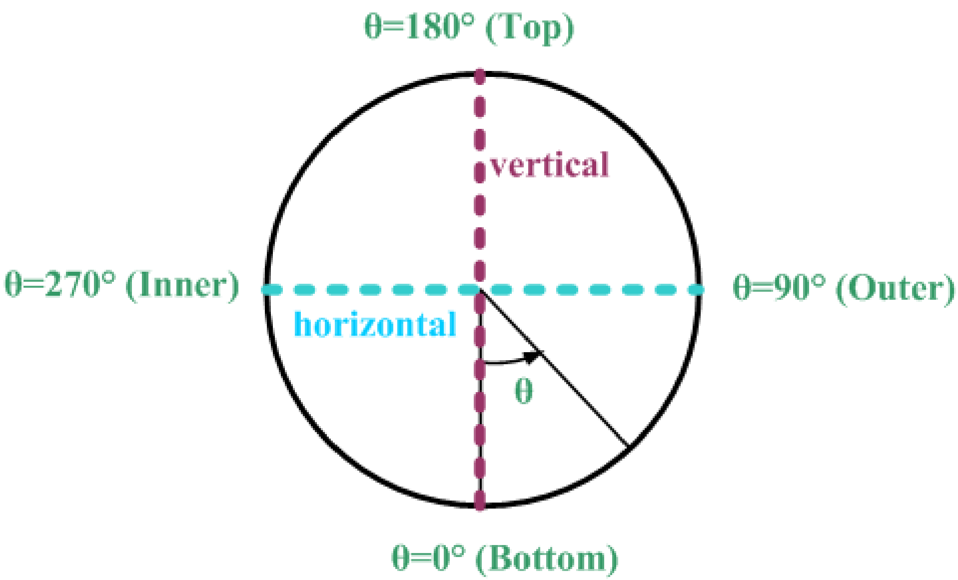

Fig. Two shown planes at the pipe outlet

Pipes	I_{mean} at outlet
$90^0/90^0$	5.204039%
$60^0/60^0$	5.323943%
$30^0/30^0$	5.368109%
$0^0/0^0$	4.649036%

Table. Mean turbulence level at pipe outlet

Mean I_{in}=4.600041%

Mercury Flow in Curved Pipes (4)

- Turbulence Level (2)

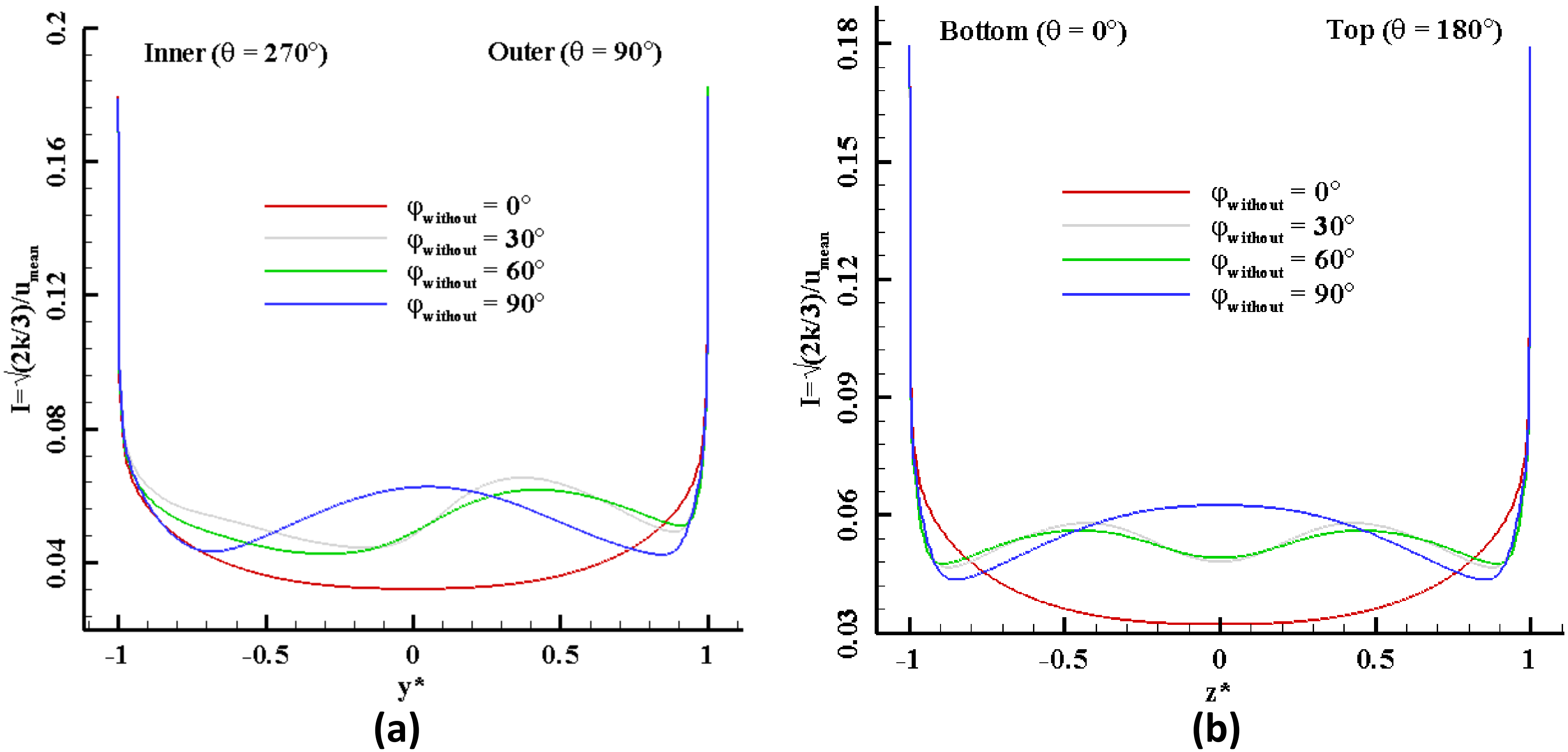

Turbulence intensity distribution at the pipe exit

(a) Horizontal plane (from inner side to outer side)

(b) Vertical (from bottom to top)

Mercury Flow in Curved Pipes (4)

- Momentum Thickness

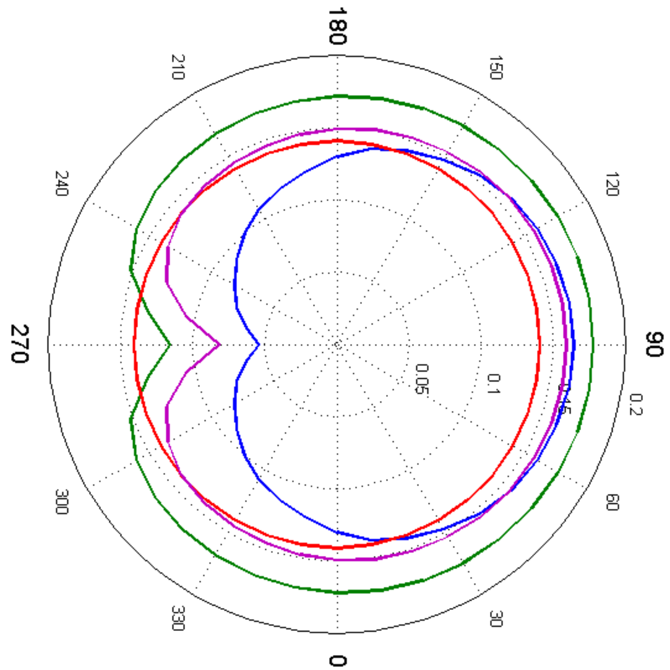

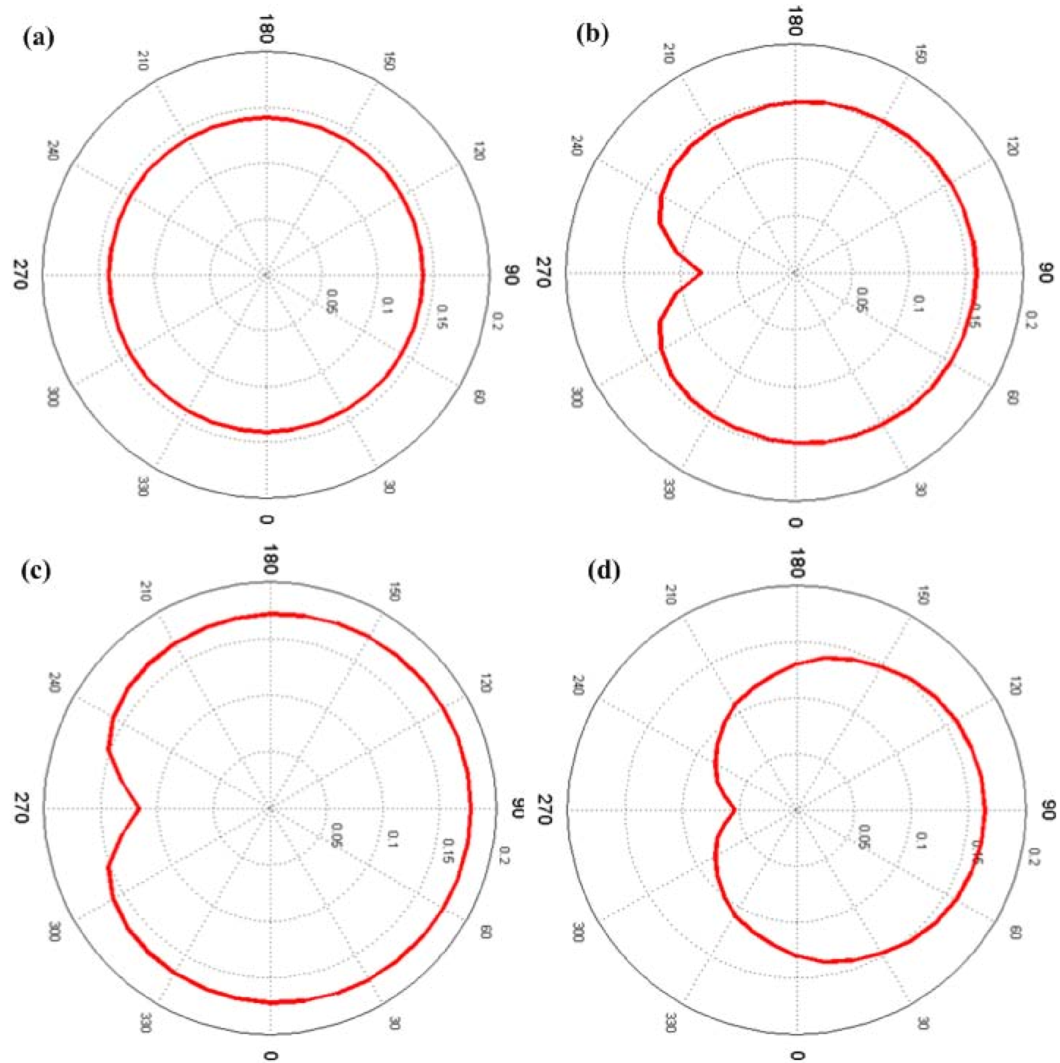

Momentum thickness distribution along the wall at the pipe exit
(a) 0º/0 º bend (b)30º/30 º bend
(c) 60º/60 º bend (d) 90º/90 º bend

Discussions

- Bend Effects
  - Bend and turbulence level
    - Bend enhances the turbulence level but not too much;
      - The $0^o/0^o$ bend has the lowest turbulence level;
    - Symmetry I for the $90^o/90^o$ bend;
  - Bend and θ_t
    - Bend effects θt not linearly with the increasing bends
      - The $60^o/60^o$ bend seems like a turning point
    - Less uniform θ_t distribution in larger bend
      - θ_t is bigger near the inner side and smaller near the outer side

Outlines

- Region of interests
- Bend Combinations without nozzle
  - Bend Combinations Without Nozzle
  - Turbulence Model Comparisons
  - Mercury Flow in Curved Pipes
  - Discussions
- Bend Combinations with Nozzle
  - Bend Combinations With Nozzle
  - Mercury Flow in Curved Nozzle Pipes
  - Discussions
- Appendix

Bend Combinations With Nozzle

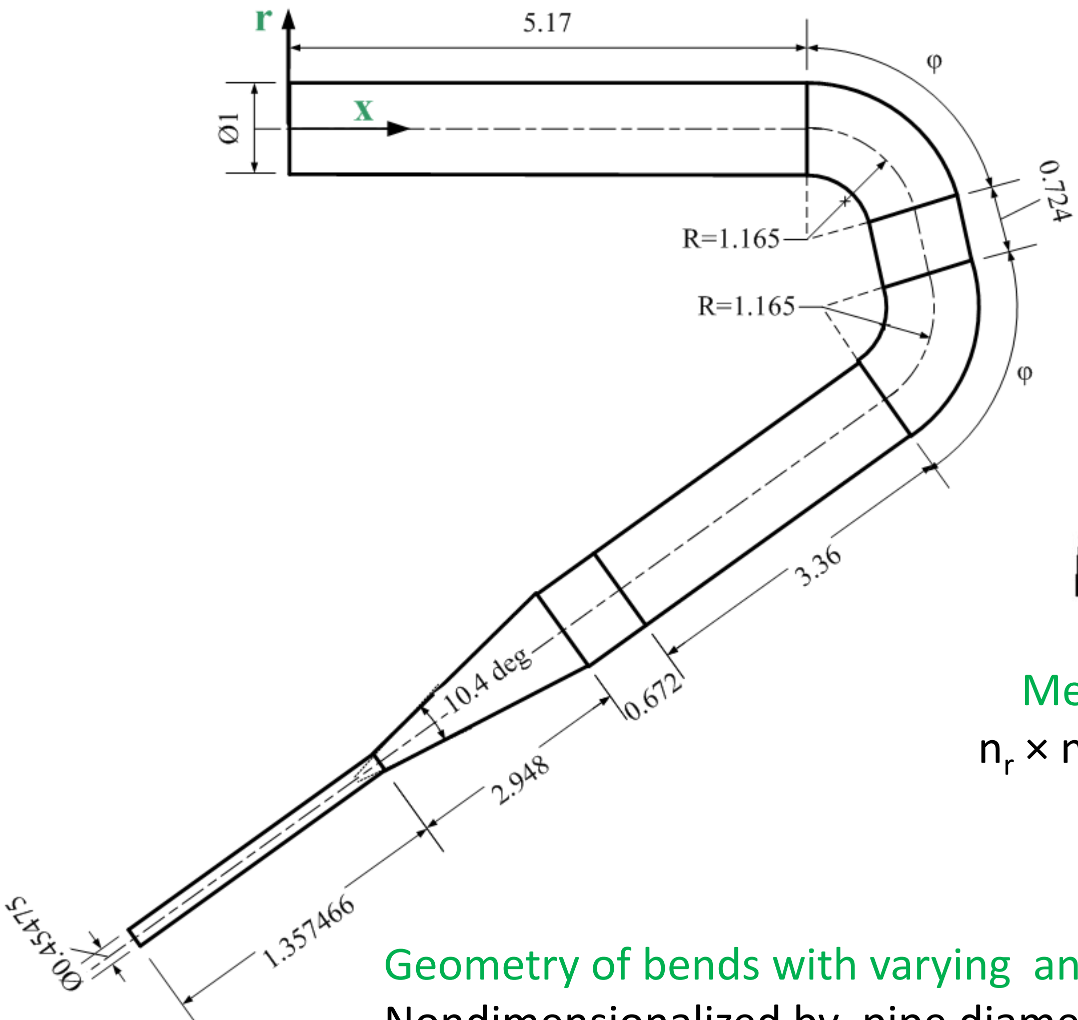

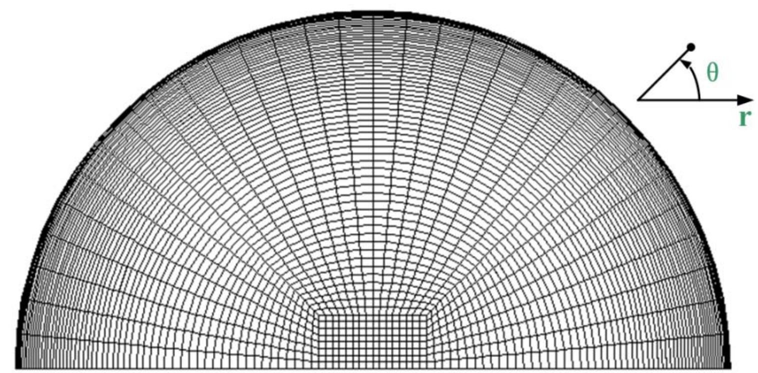

Mesh at the cross-section (half model)

$n_r \times n_\theta$ =152×64 (the 1st grid center at $y^+ \approx 1$)

Geometry of bends with varying angles

Nondimensionalized by pipe diameter (p.d.);

ϕ range: 0º, 30º, 60º, 90º.

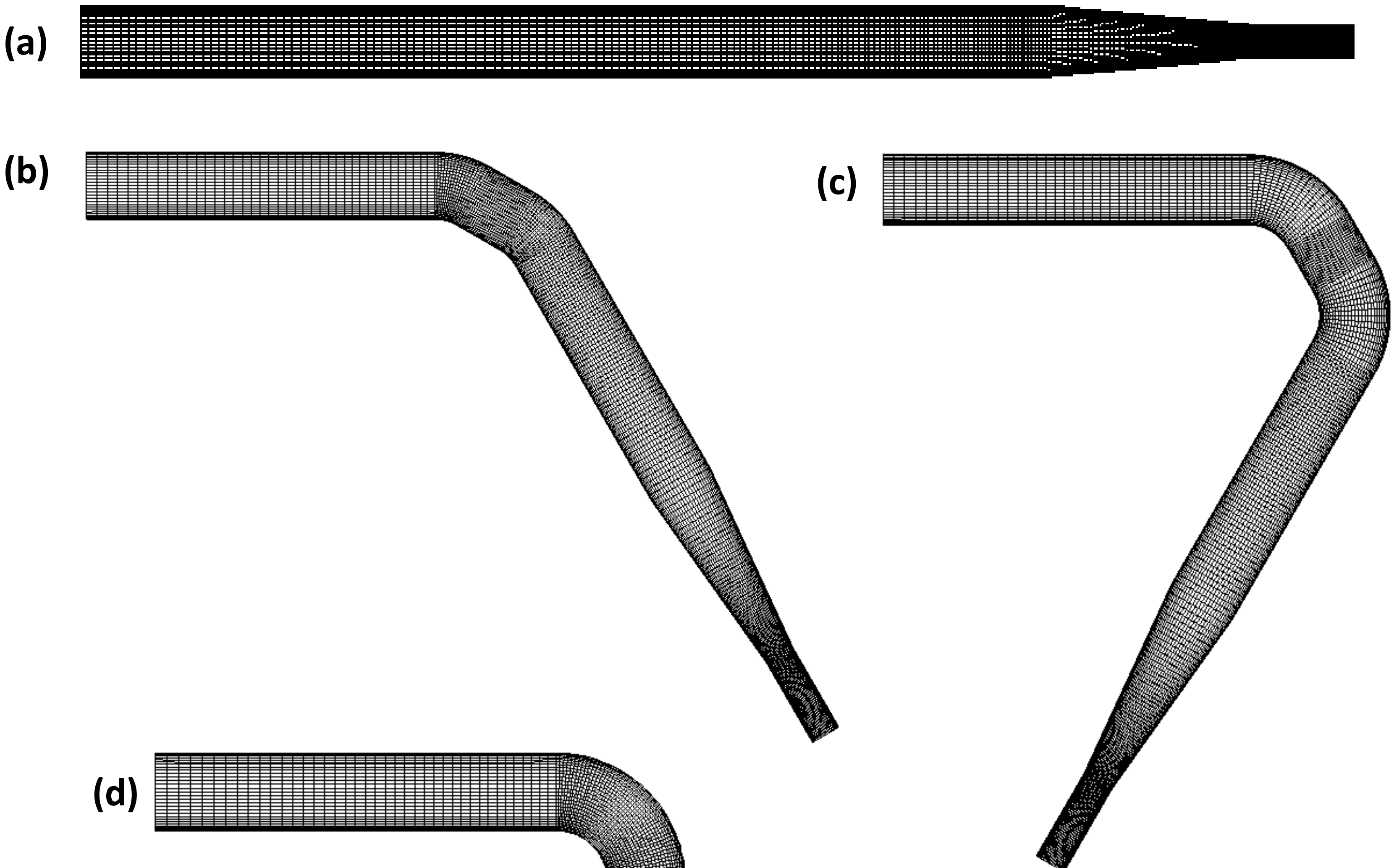

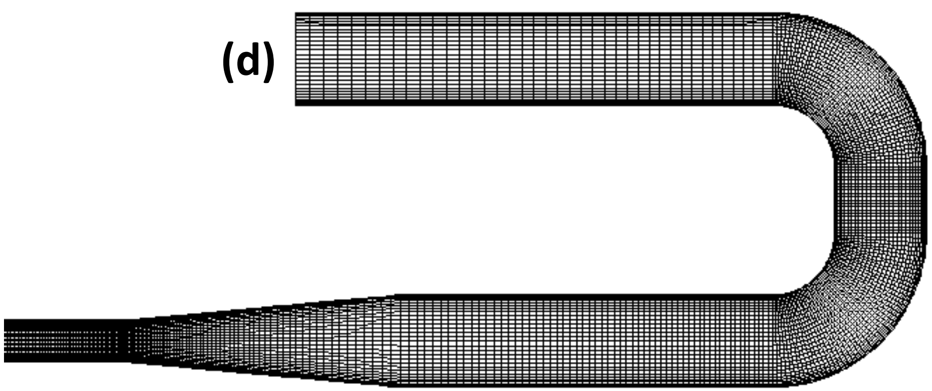

Mesh for bends

(a) 0º/0º ; (b) 30º/30º; (c) 60º/60º; (d) 90º/90º

$n_x = 40 + n_\phi + 20 + n_\phi + 60 + 70$

where n_ϕ depends on the bend angle ϕ

Mercury Flow in Curved Nozzle Pipes (1)

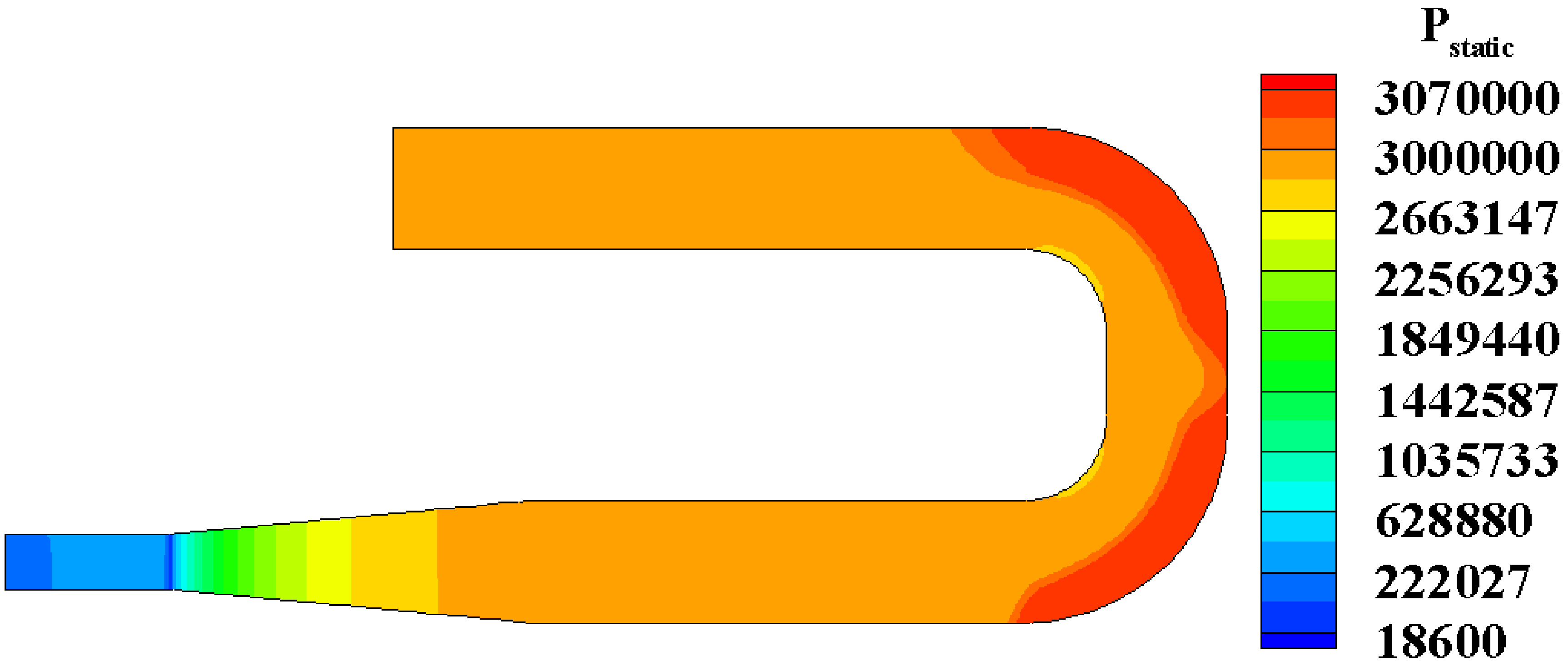

Longitudinal distribution of static pressure for 90°/90° Combination

Velocity inlet condition

P_{in} 30bar;

u_{in} fully developed velocity profile;

Outlet flow condition

Mercury Flow in Curved Nozzle Pipes (2)

- Main Loss

$$P_{main} = (\lambda l / d)_{out} \rho u_{out}^2 / 2 + (\lambda L / D)_{in} \rho u_{in}^2 / 2$$

Assume smooth pipe, thus $P_{main}=0$

- Minor Loss
  - Elbow Loss

$$h_{elbow} = \xi u_{in}^2 / 2g = 0.3 \times 4.136^2 \div 9.8 \div 2 = 0.2618\, m$$

  - Contraction Loss

$$h_{contr} = K u_{out}^2 / 2g = 0.0475 \times 20^2 \div 9.8 \div 2 = 0.9694\, m$$

- Total Loss

$$P_{loss} = P_{main} + \rho g (2h_{elbow} + h_{contr}) = 198196944 \text{ Pa}$$

Mercury Flow in Curved Nozzle Pipes (3)

- Bernoulli's Law

$$P_{in} + 0.5\rho u_{in}^2 / 2 + \rho g h_1 = P_{out} + 0.5\rho u_{out}^2 / 2 + \rho g h_1 + P_{loss}$$
$$3\times 10^6 + 4.136^2 \times 13546 \times 0.5 = P_{out} + 20^2 \times 13546 \times 0.5 + 198196.944$$
$$\Rightarrow P_{out} = 208465.3534 \text{ Pa}$$

- Comparison

$$Error = \left| \frac{P_{num} - P_{ana}}{P_{ana}} \right| \times 100\%$$
$$= \left| \frac{189516.3 - 208465.3534}{208465.3534} \right| \times 100\% = 9.0898\%$$

Mercury Flow in Curved Nozzle Pipes (4)

- Turbulence Level (1)

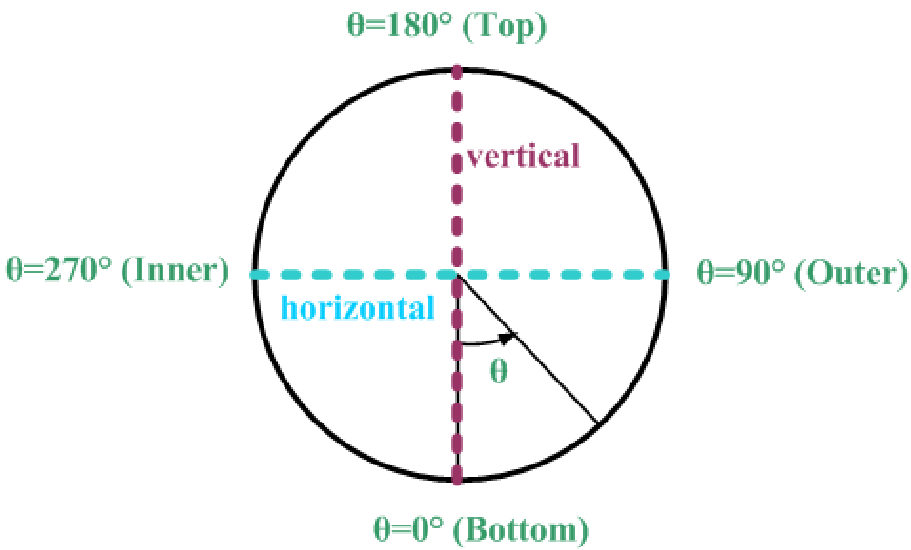

Fig. Two shown planes at the pipe outlet

Pipes	I_{mean} (Nozzle)	I_{mean} (No nozzle)
$90^0/90^0$	5.143341%	5.204039%
$60^0/60^0$	2.858747%	5.323943%
$30^0/30^0$	2.701366%	5.368109%
$0^0/0^0$	2.182027%	4.649036%

Table. Mean turbulence level at pipe outlet

Mean I_{in}=4.599195%

Mercury Flow in Curved Nozzle Pipes (5)

- Turbulence Level (2)

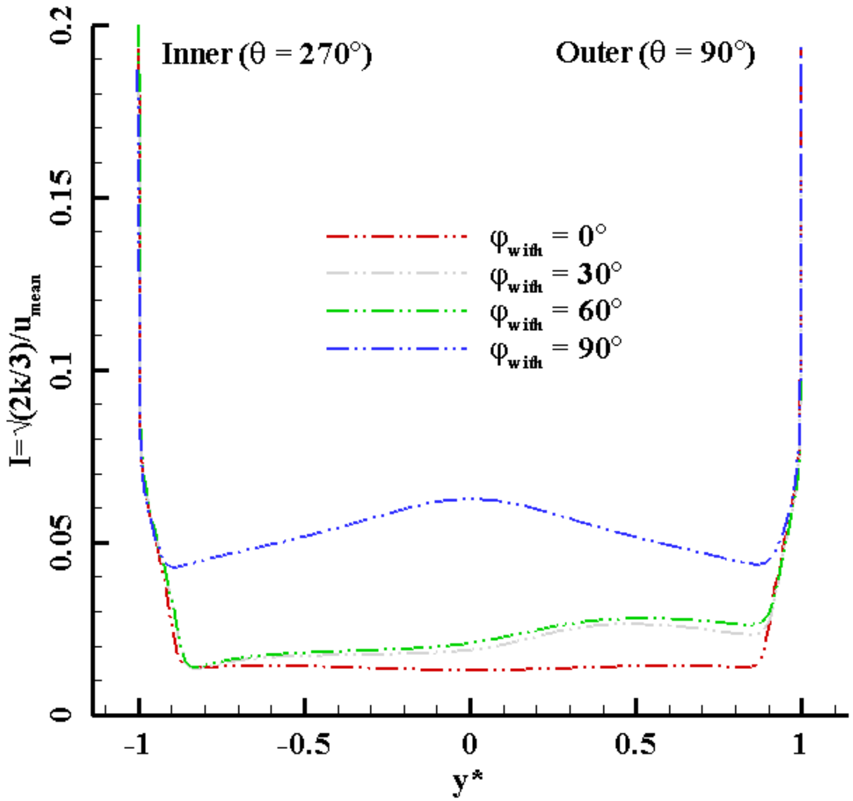

(a)

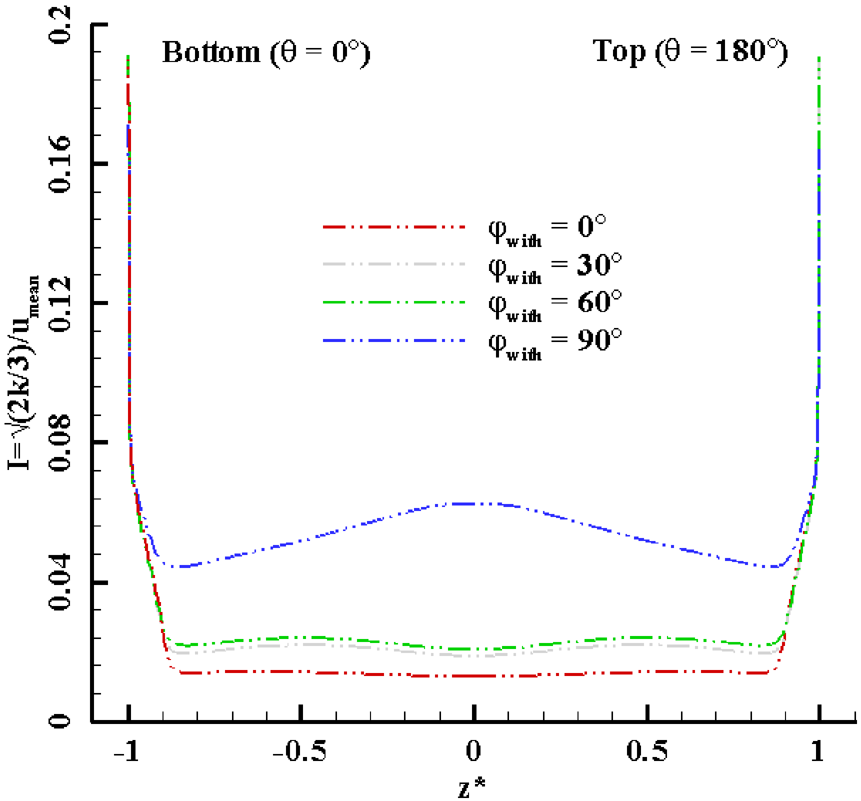

(b)

Turbulence intensity distribution at the pipe exit

(a) Horizontal plane ; (b) Vertical plane

Mercury Flow in Curved Pipes (6)

- Momentum Thickness

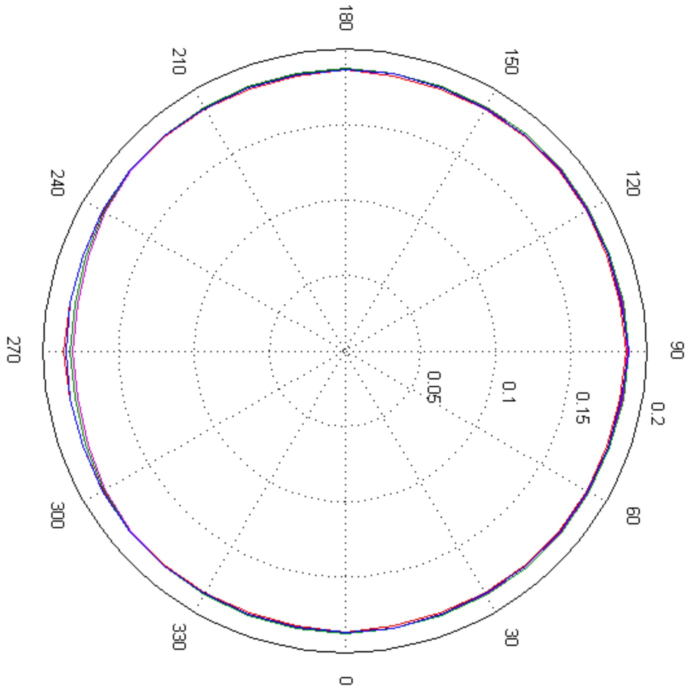

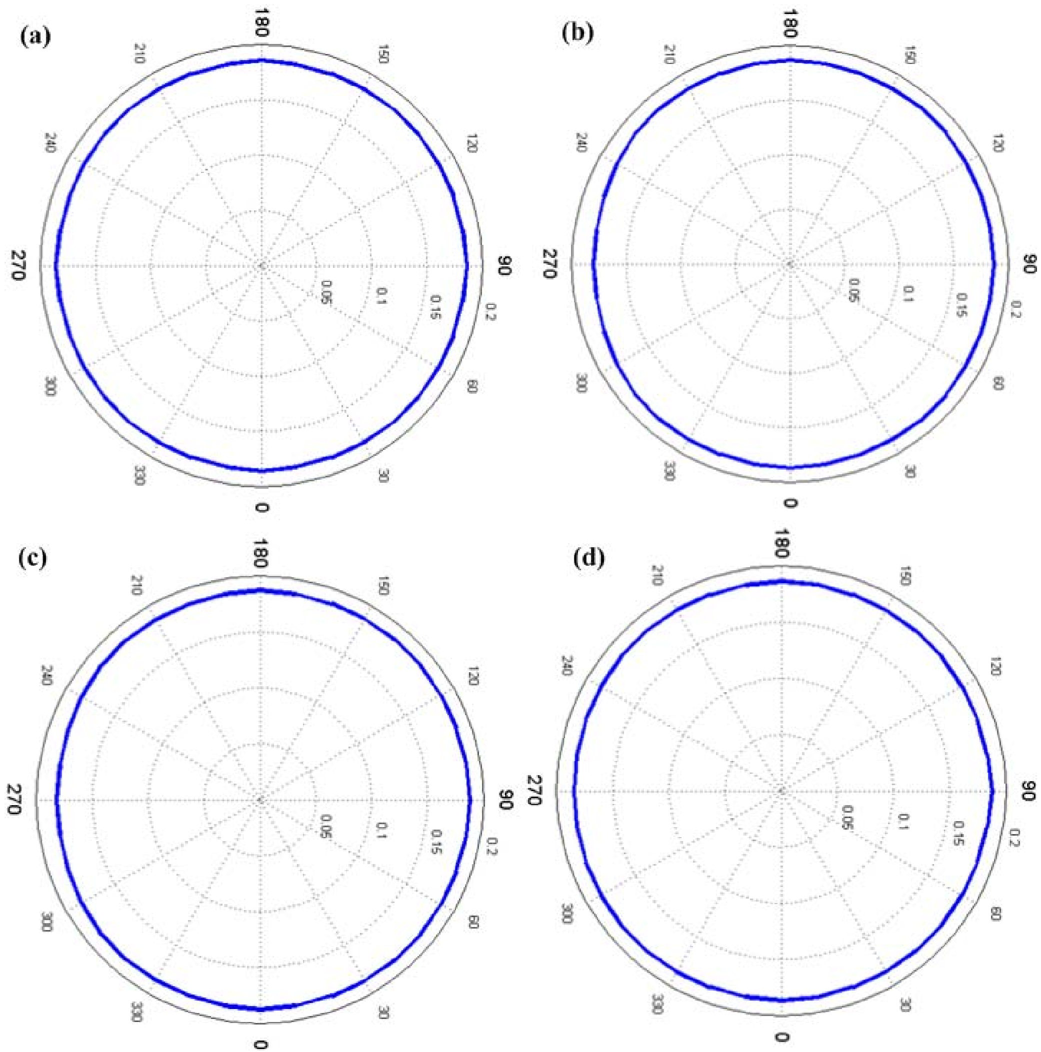

Momentum thickness distribution along the wall at the pipe exit
(a) 0º/0 º bend (b)30º/30 º bend
(c) 60º/60 º bend (d) 90º/90 º bend

Discussions (1)

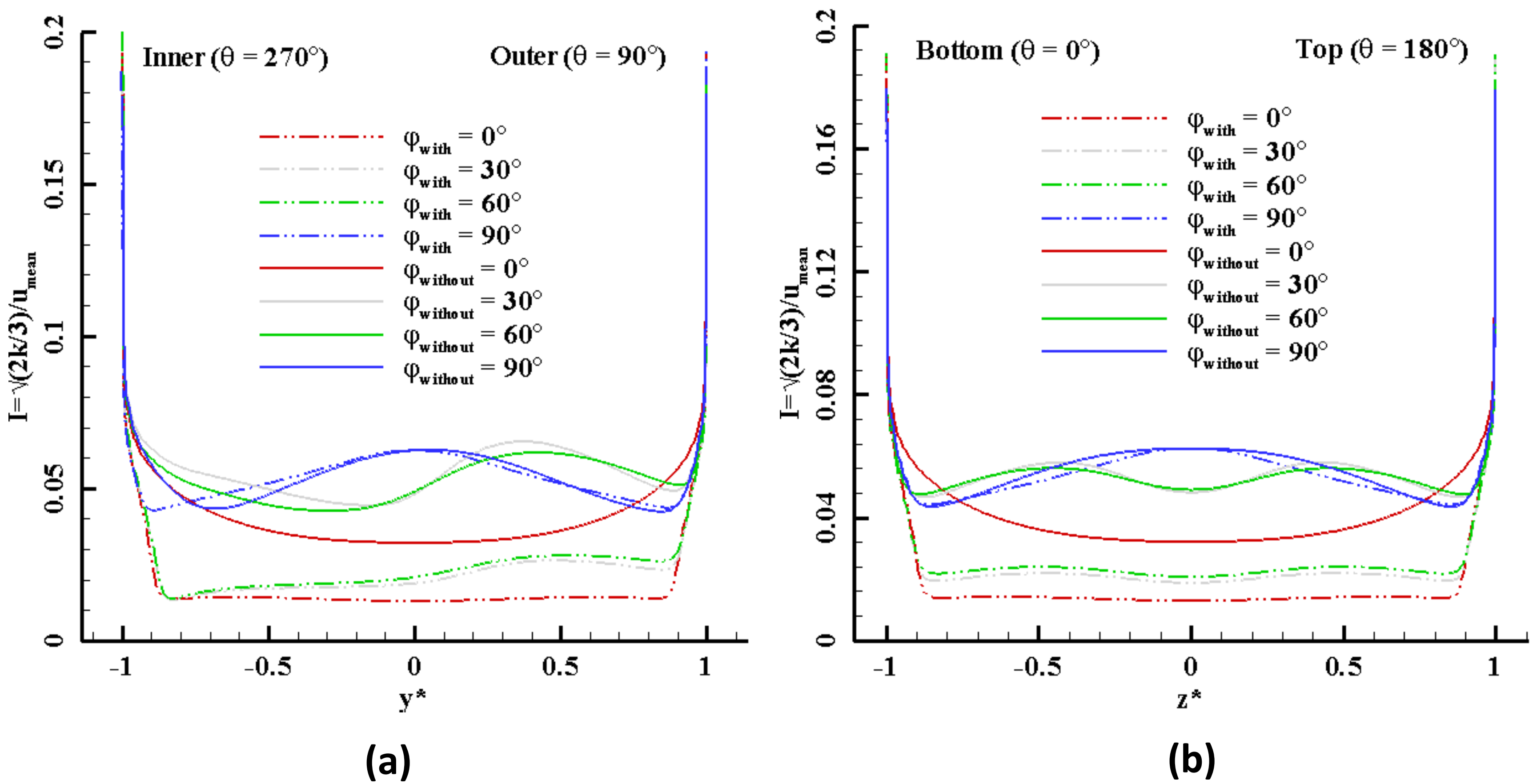

Turbulence intensity distribution at the pipe exit
(a) Horizontal plane (b)Vertical plane

Discussions (2)

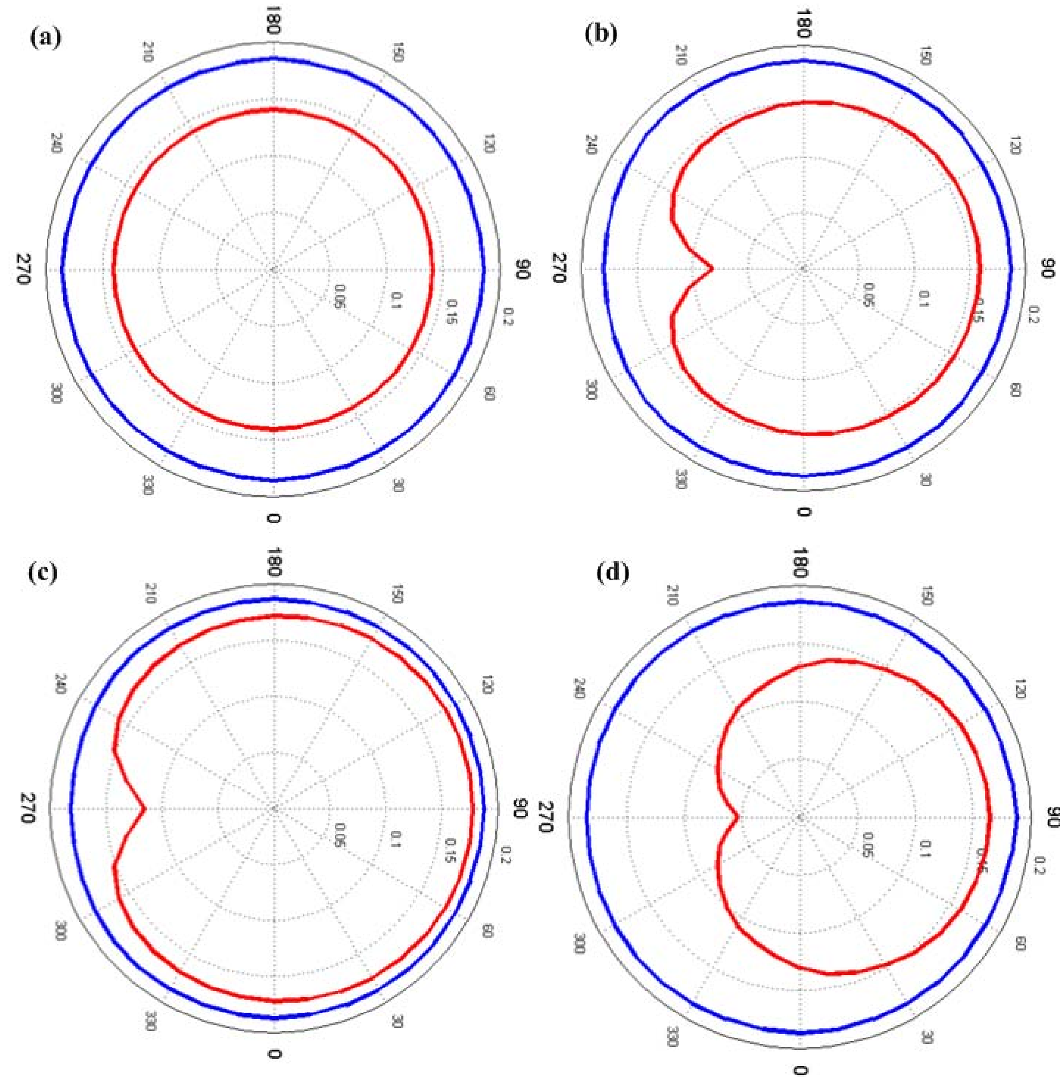

The comparison of momentum thickness distribution at the pipe exit between pipe with/without nozzle

(a) 0º/0 º bend (b)30º/30 º bend

(c) 60º/60 º bend (d) 90º/90 º bend

Red: pipe without nozzle;

Blue: pipe with nozzle.

Discussions (3)

- Nozzle Effects
  - Nozzle and turbulence level
    - Nozzle reduces the turbulence level;
      - The $90^o/90^o$ bend doesn't change too much;
    - I of the $90^o/90^o$ bend is far different from other bends
  - Nozzle and θ_t
    - Nozzle decreases θt
    - Very uniform and similar θ_t distribution at the nozzle exit for all bend pipes

Outlines

- Region of interests
- Bend Combinations without nozzle
  - Bend Combinations Without Nozzle
  - Turbulence Model Comparisons
  - Mercury Flow in Curved Pipes
  - Discussions
- Bend Combinations with Nozzle
  - Bend Combinations With Nozzle
  - Mercury Flow in Curved Nozzle Pipes
  - Discussions
- Appendix

Appendix(1)

- ## Continuity Equation

The two-phase model considers mixture comprising of liquid, vapor and non-condensable gas (NCG). Gas is compressible, the liquid and vapor are impressible. The mixture is modeled as incompressible.

$$\frac{\partial u_j}{\partial x_j} = 0$$

- ## Momentum Equations

$$\rho \frac{\partial u_i u_j}{\partial x_j} = -\frac{\partial P}{\partial x_i} + \frac{\partial \tau_{ij}}{\partial x_j}$$

$$\text{where } \tau_{ij} = (\mu + \mu_t)\{\frac{\partial u_i}{\partial x_j} + \frac{\partial u_j}{\partial x_i}\} \text{ and } \mu_t = C_\mu \rho (\frac{k^2}{\varepsilon})$$

Appendix(2)

- Spalart-Allmaras Model

$$\frac{\partial \rho u_i \tilde{\nu}}{\partial x_i} = G_\nu + \frac{1}{\sigma_{\tilde{\nu}}}[\frac{\partial}{\partial x_j}\{(\mu + \rho\tilde{\nu})\frac{\partial \tilde{\nu}}{\partial x_j}\} + C_{b2}\rho(\frac{\partial \tilde{\nu}}{\partial x_j})^2] - Y_\nu + S_{\tilde{\nu}}$$

The production term $G_\nu = C_{b1}\rho\tilde{S}\tilde{\nu}$ and $\tilde{S} \equiv S + \tilde{\nu} f_{\tilde{\nu}2} / (\kappa^2 d^2)$

where $f_{\tilde{\nu}2} = 1 - \chi/(1 + \chi f_{\tilde{\nu}1})$ and $S \equiv \sqrt{2\Omega_{ij}\Omega_{ij}}, \Omega_{ij} = (u_{i,j} - u_{j,i})/2$

The destruction term $Y_\nu = C_{w1}\rho f_w (\tilde{\nu}/d)^2$

where $f_w = g[(1 + C_{w3}^6)/(g^6 + C_{w3}^6)]^{1/6}, g = r + C_{w2}(r^6 - r), r \equiv \tilde{\nu}/(\tilde{S}\kappa^2 d^2)$

$C_{b1} = 0.1355, C_{b2} = 0.622, \kappa = 0.4187, \sigma_{\tilde{\nu}} = 2/3, C_{v1} = 7.1, C_{w2} = 0.3$

$C_{w3} = 2.0, C_{w1} = C_{b1}/\kappa^2 + (1 + C_{b2})/\sigma_{\tilde{\nu}}$

User-defined source term S_ν, ignored estimating the Reynolds stresses

Appendix(3)

- Turbulent Viscosity (SA)

$$\mu_t = \rho \tilde{v} f_{\tilde{v}1}$$

where visous damping function $f_{\tilde{v}1} = \dfrac{\chi^3}{\chi^3 + C_{\tilde{v}1}^3}$ and $\chi \equiv \tilde{v} / v$

v is the molecular kinematic viscosity.

Appendix (4)

- Standard K-ε model

$$\frac{\partial \rho k}{\partial t}+\frac{\partial \rho u_j k}{\partial x_j}=\frac{\partial}{\partial x_j}[(\mu+\frac{\mu_t}{\sigma_k})\frac{\partial k}{\partial x_j}]+G_k+G_b-\rho\varepsilon-Y_M+S_k$$

$$\frac{\partial \rho \varepsilon}{\partial t}+\frac{\partial \rho u_j \varepsilon}{\partial x_j}=\frac{\partial}{\partial x_j}[(\mu+\frac{\mu_t}{\sigma_\varepsilon})\frac{\partial \varepsilon}{\partial x_j}]+C_{1\varepsilon}\frac{\varepsilon}{k}(G_k+C_{3\varepsilon}G_b)-C_{2\varepsilon}\rho\frac{\varepsilon^2}{k}+S_\varepsilon$$

$$G_k=-\rho\overline{u_i'u_j'}\frac{\partial u_j}{\partial x_i}, G_b=\beta g_i\frac{\mu_t}{\Pr_t}\frac{\partial T}{\partial x_i}, Y_M=2\rho M_t^2, M_t=\sqrt{\frac{k}{\gamma RT}}$$

$$C_{1\varepsilon}=1.44, C_{2\varepsilon}=1.92, C_\mu=0.09, \sigma_k=1.0, \sigma_\varepsilon=1.3$$

Appendix (5)

- Turbulent Viscosity (SKε)

$$\mu_t = \rho C_\mu \frac{k^2}{\varepsilon}$$

C_μ is a constant.

G_k : generation of k due to mean velocity gradients;

G_b : generation of k due to buoyance;

Y_M : contribution of the fluctuating dilatation in compressible turbulence to the overall dissipation rate;

$\sigma_k, \sigma_\varepsilon$: turbulent Prandtl numbers for k and ε;

S_k, S_ε : user - defined source terms;

Appendix (6)

- Realizable K-ε model

$$\frac{\partial \rho k}{\partial t}+\frac{\partial \rho u_j k}{\partial x_j}=\frac{\partial}{\partial x_j}[(\mu+\frac{\mu_t}{\sigma_k})\frac{\partial k}{\partial x_j}]+G_k+G_b-\rho\varepsilon-Y_M+S_k$$

$$\frac{\partial \rho \varepsilon}{\partial t}+\frac{\partial \rho u_j \varepsilon}{\partial x_j}=\frac{\partial}{\partial x_j}[(\mu+\frac{\mu_t}{\sigma_\varepsilon})\frac{\partial \varepsilon}{\partial x_j}]+C_1\rho S\varepsilon-C_2\rho\frac{\varepsilon^2}{k+\sqrt{v\varepsilon}}+C_{1\varepsilon}\frac{\varepsilon}{k}C_{3\varepsilon}C_b+S_\varepsilon$$

$$C_1=\max[0.43,\frac{\eta}{\eta+5}],\eta=S\frac{k}{\varepsilon},S=\sqrt{2S_{ij}S_{ij}}$$

$$G_k=-\rho\overline{u_i'u_j'}\frac{\partial u_j}{\partial x_i},G_b=\beta g_i\frac{\mu_t}{\Pr_t}\frac{\partial T}{\partial x_i},Y_M=2\rho M_t^{\ 2},M_t=\sqrt{\frac{k}{\gamma RT}}$$

Appendix (7)

- Turbulent Viscosity (RKε)

$$\mu_t = \rho C_\mu \frac{k^2}{\varepsilon}$$

$$C_\mu = \frac{1}{A_0 + A_s \dfrac{kU^*}{\varepsilon}}, U^* \equiv \sqrt{S_{ij}S_{ij} + \tilde{\Omega}_{ij}\tilde{\Omega}_{ij}}, \tilde{\Omega}_{ij} = \Omega_{ij} - 2\varepsilon_{ijk}\omega_k, \Omega_{ij} = \overline{\Omega}_{ij} - \varepsilon_{ijk}\omega_k$$

$$A_0 = 4.04, A_s = \sqrt{6}\cos\phi, \phi = \frac{\cos^{-1}(\sqrt{6}W)}{3}, W = \frac{S_{ij}S_{jk}S_{ki}}{\tilde{S}^3}, \tilde{S} = \sqrt{S_{ij}S_{ji}}$$

$$S_{ij} = \frac{u_{ij} + u_{ji}}{2}, C_{1\varepsilon} = 1.44, C_2 = 1.9, \sigma_k = 1.0, \sigma_\varepsilon = 1.2$$

Appendix(8)

Models	Pros	Cons
Spalart-Allmaras (SA)	Low-cost; Aerospace applications involving wall-bounded flows and with mild separation;	Can not predict the decay of homogeneous, isotropic turbulence; No claim is made regarding its applicability to all types of complex engineering flows;
Standard K-ε (Skε)	Robust and reasonably accurate; Most widely-used engineering model industrial applications; Contains submodels for buoyancy, compressibility, combustion, etc;	Must use wall function for near wall calculation; Performs poorly for flows with strong separation, large streamline curvature, and large pressure gradient;
Realizable K-ε (Rkε)	superior performance for flows involving rotation, boundary layers under strong adverse pressure gradients, separation, and recirculation	

Appendix (9)

- Properties of fluid

Variable Values	
Pipe ID	0.884 inch
Nozzle exit ID	0.402 inch
Driving pressure	30 bar
Frequency for Hg supply	12 s
Maximum Cycles	100
Jet Velocity	20 m/s
Jet Diameter	1 cm
Jet Flow rate	1.6 L/sec
Environment	1 atm air /vacuum

Mercury Properties (25 ^{0}C)	
Density	13.546 kg/L
Sound Speed	1451 m/s
Bulk Modulus	2.67×10^{10}Pa
Dynamic Viscosity	1.128×10^{-7} m^2/s
Thermal Conductivity	8.69 W/m·K
Electrical Conductivity	10^6 Siemens/m
Specific Heat	0.139 J/kg·K
Prandtl Number	0.025
Surface Tension	465 dyne/cm

- Steady incompressible turbulent flow